ACS Sustainable Chemistry & Engineering

Research Article

pubs.acs.org/journal/ascecg

Green Recovery of Rare Earths from Waste Cathode Ray Tube Phosphors: Oxidative Leaching and Kinetic Aspects

Xiaofei Yin,[†,‡] Yufeng Wu,[*,†,‡] Xiangmiao Tian,[†,‡] Jiamei Yu,[*,†,‡] Yi-Nan Zhang,[§] and Tieyong Zuo[†,‡]

[†]Institute of Circular Economy, Beijing University of Technology, Beijing, 100124, P. R. China

[‡]Institute of Beijing-Tianjin-Hebei Green Development, Beijing University of Technology, Beijing, 100124, P. R. China

[§]Institute of Biomaterials and Biomedical Engineering, University of Toronto, Toronto, Ontario M5S 3G9, Canada

Supporting Information

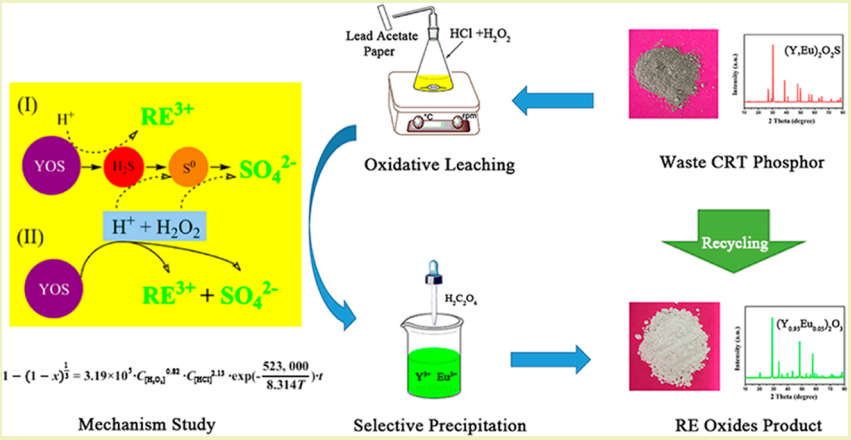

ABSTRACT: In this work, we developed a green and efficient process for the recovery of rare earths from waste cathode ray tube phosphors. The mixture of hydrochloric acid and hydrogen peroxide was identified as the most suitable leaching agent due to the synergistic effect. The effects of various parameters on leaching process were explored, and the optimal conditions with stirring speed 600 rpm, temperature 313 K, 1 M of H_2O_2, 4 M of HCl, and leaching time of 90 min were determined. Furthermore, a possible reaction mechanism was proposed, and the kinetics for the leaching process was investigated in detail. The leaching process was found to follow a shirking-core model, with the chemical reaction as the rate-controlling step. The apparent activation energy of the reaction was calculated as 52.3 kJ/mol, and the reaction orders for H_2O_2 and HCl were established as 0.82 and 2.13, respectively. The kinetic equation was established. Moreover, the optimal leaching conditions were applied to the waste phosphors, and the oxalate precipitation process was employed, achieving the recovery rate of rare earths >99.5%. After calcining, a well crystallized $(Y_{0.95}Eu_{0.05})_2O_3$ product with a purity of 99% was obtained with an average diameter of 5 μm.

KEYWORDS: *Waste CRT phosphor, Recycling, Rare earths, Oxidative leaching, Kinetics*

1. INTRODUCTION

Trivalent europium doped yttrium oxysulifde $Y_2O_2S:Eu^{3+}$ (YOS) is a common red emitting phosphor which has been widely used in cathode ray tubes (CRTs) and field emission displays (FEDs).[1−4] With the rapid development of modern display industry, a considerable number of waste CRTs are generated every year.[5] Statistics showed that approximately 5.96 million units of CRT computer monitors and TVs were obsoleted every year in North America[6] and that more than 60 million accumulated in China in 2013.[7] There are about 1−7 g of phosphor in a certain unit CRT, in which the rare earths (RE) accounts for 15% approximately.[8−10] Previously, the collection and recycling of waste CRTs have so for usually focused on the disposal and the reutilization of lead (Pb) contained in the CRT glass.[11] However, the waste CRT phosphors (WCP) are not recycled but discarded, landfilled, or stockpiled as hazardous materials, which not only causes loss of RE resources but also brings about environmental pollution due to the contents of toxic heavy metals such as cadmium (Cd) and Pb in WCP. Considering the availability and supply risk of the critical raw material,[12] waste rare earth phosphors have been viewed as a potential urban mining resource for rare earth recovery.

Waste lamp phosphors have been already investigated and recycled successfully by scientists from all over the world.[13,14] While in contrast, only few previous works were focused on

Received: August 16, 2016
Revised: September 16, 2016
Published: September 21, 2016

DOI: 10.1021/acssuschemeng.6b01965
ACS Sustainable Chem. Eng. 2016, 4, 7080−7089

recycling phosphors from waste CRTs. Morais et al.[8,9] studied the recovery of REs from waste computer monitor phosphors. Concentrated sulfuric acid was chosen as the leaching reagent, a sulfuric acid/sample ratio of 1250 g/kg was used for the dissolution, and hydrogen sulfide (H_2S) and sulfur dioxide (SO_2) were discharged in the process. Innocenzi et al.[15] focused their work on the recovery of yttrium and zinc from WCP. The leaching rate of yttrium and zinc reached 100% in liquid containing sulfuric acid and H_2O_2, both elemental sulfur and SO_2 were generated unavoidably. However, these methods were often limited, due to the high temperature involved in the leaching processes, and the toxic and dangerous gases were released during leaching such as H_2S and SO_2. High energy consumption and pollutant discharge are contrary to the concept of the principle of "3R". In addition, no studies have investigated the kinetics of leaching process. Thus, it is necessary to find a green recovery process and fill the lack of fundamental research knowledge about the leaching mechanism.

The present work focuses on exploring a green and efficient recycling process of rare earths from waste CRT phosphors. First, a high-efficiency, low-cost, and pollution-free leaching reagent was selected; in addition, the effects of variables such as stirring speed, temperature, and regent concentration on the leaching rate were investigated. Then, the reaction mechanism and leaching kinetics were explored systematically. Finally, rare earth products were recycled by selective precipitation.

2. EXPERIMENTAL SECTION

2.1. Materials. All reagents used in this study were of the highest available purity, purchased from Chemical Reagent Company of Beijing. Deionized water (18.2 MΩ·cm) obtained from a Direct-Pure Up 10 water system (RephiLe Bioscience, Ltd.) was used through the experiments whenever needed. The pure red phosphor ($Y_2O_2S:Eu^{3+}$) was purchased from Grirem Advanced Materials Co., Ltd. (Beijing, China). The waste CRT phosphors used in this study were collected from typical CRT after dismantled, which were supplied by Changzhou Xiangyu Resource Recycling Technology Co., Ltd. (Changzhou, China). The waste CRT phosphors have been pretreated for removing impurities, and the detailed information about the compositions and XRD patterns are given in section I (Table S1 and Figure S1) in the Supporting Information (SI).

2.2. Apparatus. The powder composition was analyzed by X-ray fluorescence (XRF, PW2403, PANalytical, Holland). The mineralogical analysis of the sample was carried out in an X-ray diffractomer (XRD) with a Bruker Axs D8 Advance using Cu Ka radiation (Bruker, Germany). The morphology of the sample was examined by SU-8000 field-emission scanning electron microscopy (SEM) with an Energy Dispersive Spectrometer (EDS) system (Hitachi, Japan). Analyses of rare earth in solutions were performed by Inductively Coupled Plasma Optical Emission Spectrometer (ICP-OES, Optima 8000, PerkinElmer, Shelton, CT 06484, USA).

2.3. Methodology. The process described in this article aims to describe recycling rare earths from waste CRT phosphors by oxidative leaching and selective precipitation, and the leaching kinetics were highlighted investigated (Figure 1). Our initial research focused on identifying an appropriate leaching reagent for complete dissolution of rare earths from waste CRT phosphors employing strategies that are environmentally friendly, energy-efficient, and economical. Pure and unmixed red phosphors (YOS) were employed for the investigation of dissolution characteristics and kinetics study. The effect of stirring speed, temperature, and reagent concentration on the leaching process were explored and optimized systematically. In most leaching experiments, the tapered glass vials (50 mL) were used as reaction vessels. The samples mixed with desired reagents were stirred at appropriate temperatures with a solid/liquid ratio of 25 g/L for a certain time. The lead acetate papers were used for detecting hydrogen sulfide. The leachate was filtrated into volumetric flasks to determine the RE concentration in solution by ICP-OES. The kinetics mechanism of YOS dissolution was established. Moreover, the optimized leaching conditions were verified by the real waste CRT phosphor. Finally, selective precipitation of RE salts was followed, resulting in RE oxides products.

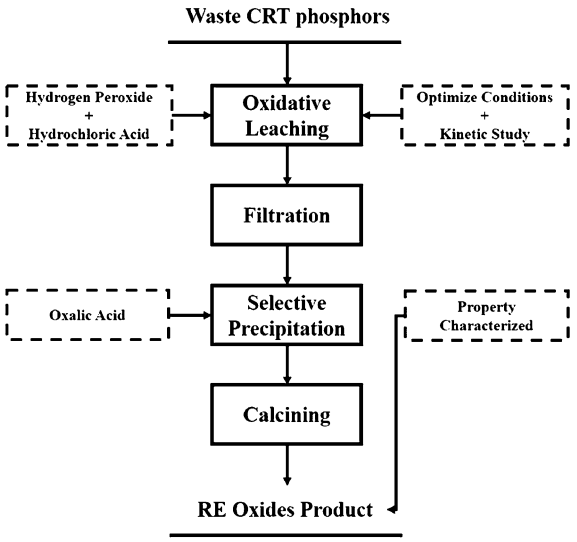

Figure 1. Flowchart of rare earth recycling from waste CRT phosphors.

3. RESULTS AND DISCUSSION

3.1. Selection of Appropriate Leaching Reagents. Hydrochloric acid (HCl), sulfuric acid (H_2SO_4), nitric acid (HNO_3), and hydrogen peroxide (H_2O_2, 30%) which can be produced abundantly with low prices were employed as leaching reagents. Hydrogen peroxide as a strong oxidant is an environmentally safe reagent since only water was generated during oxidation of sulfide minerals.[16] For the purpose of comparison, six dissolution systems including HNO_3, H_2SO_4, H_2SO_4 + H_2O_2, HCl, HCl + H_2O_2, and H_2O_2 were designed. All experiments were carried out at room temperature for 12h.

Figure 2 illustrates the results of different leaching reagents applied in dissolving YOS. The leaching reagents HNO_3 and H_2SO_4 were abandoned due to the low leaching efficiency and the emission of gases such as $NO_{X\,(g)}$, $SO_{2\,(g)}$, and $H_2S_{\,(g)}$. The dissolution rate of REs by H_2SO_4 + H_2O_2 reached above 98%; however, a strong odor of H_2S mixed with SO_2 was released

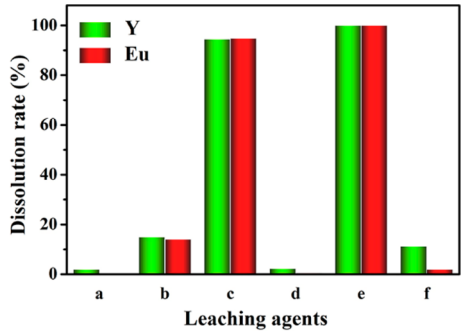

Figure 2. Dissolution of YOS employing different leaching reagents: (a) 4 M HNO_3, (b) 2 M H_2SO_4, (c) 2 M H_2SO_4 + 10% v/v H_2O_2, (d) 4 M HCl, (e) 4 M HCl + 10%v/v H_2O_2, and (f) H_2O_2.

DOI: 10.1021/acssuschemeng.6b01965
ACS Sustainable Chem. Eng. 2016, 4, 7080−7089

during leaching. In addition, some insoluble faint yellow precipitate was observed, which was supposed to be elemental sulfur. Fortunately, a complete dissolution of Y and Eu was reached using HCl + H_2O, and we also found the overwhelming majority of the S^{2-} in YOS was oxidized to be SO_4^{2-} in the leachate (detected by XRD, Figure S2). Therefore, the contamination by $H_2S_{(g)}$, $SO_{2(g)}$, and elemental sulfur residues was avoided efficiently. Comparing experiments d and e, it was obvious that hydrogen peroxide played a highly critical role in both dissolving and oxidizing, but single hydrochloric acid or hydrogen peroxide cannot dissolve YOS completely, lower than 20% (shown in Figure 2f). The results indicated that H^+ and H_2O_2 play a synergistic effect in the dissolution process. Therefore, the HCl + H_2O_2 reagent was selected as the leaching reagent. In the following step, the leaching parameters were investigated systematically.

3.2. Effect of Different Leaching Parameters. *3.2.1. Effect of Stirring Speed.* The effect of stirring speed on the dissolution of YOS was investigated in the range of 0−1200 rpm using 4 M of HCl and 1 M of H_2O_2 at room temperature. As shown in Figure 3, stirring has a positive effect on the dissolution compared with no stirring. Experiments revealed that a strong smell of hydrogen sulfide assailed the nostrils without stirring, which is likely due to the fact that HCl and H_2O_2 were not intensively mixed on the surface of YOS, and the reduction of H_2O_2 concentration in the contact surface led to the occurrence of a side reaction which produced hydrogen sulfide. As a consequence, stirring was necessary for the dissolution of YOS. While Aydogan[17] found different results for sphalerite dissolution by hydrogen peroxide in sulfuric acid, they reported that no obvious changes of the sphalerite oxidation rate occurred under the stirring speed of 0 and 300 rpm.

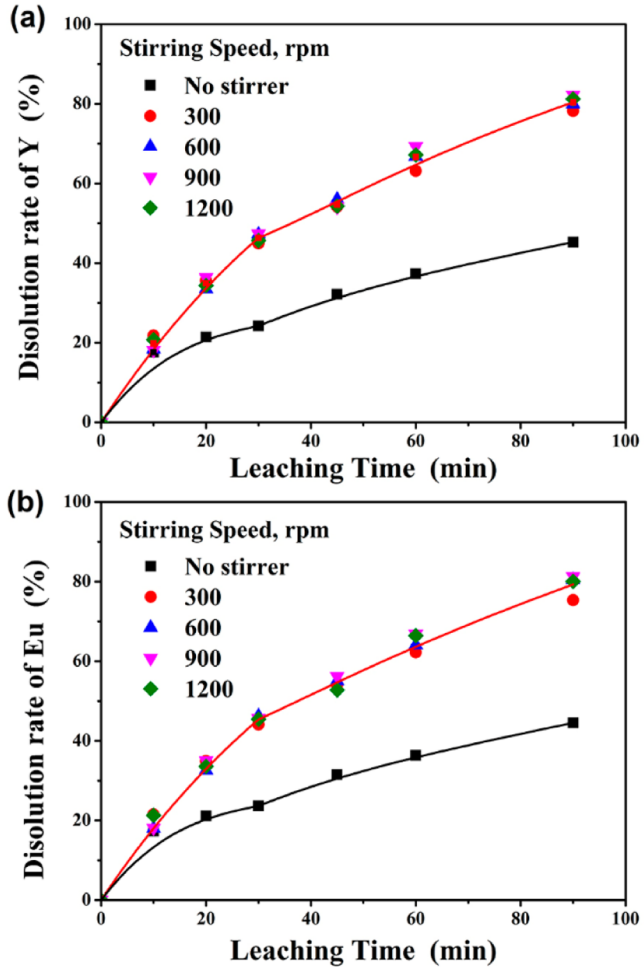

Figure 3. Effect of stirring speed on the dissolution of YOS: (a) dissolution rate of Y; (b) dissolution rate of Eu.

We also found that there was no obvious difference in the dissolution rate when stirring at 300, 600, 900, and 1200 rpm, which meant the dissolution of YOS was independent of the stirring speed. Antonijević et al.[18] found similar results for chalcopyrite dissolution by hydrogen peroxide in sulfuric acid and concluded that the leaching process was not controlled by film diffusion, and researchers[19,20] also pointed out that stirring might have a negative influence on the oxidative leaching process due to the decomposition of hydrogen peroxide or better contact between particles and peroxide in the high stirring speed. In our study, we found a very small decrease of dissolution rate took place when the stirring speed was increased to 1200 rpm. Hence, the stirring speed of 600 rpm was used for all subsequent experiments.

3.2.2. Effect of Temperature. The effect of temperature on YOS dissolution was carried out in the range of 303−333 K in solution containing 4 M of HCl and 1 M of H_2O_2 and stirring at 600 rpm. The results shown in Figure 4 indicate that the extraction of Y and Eu gradually increases with the temperature. The change of temperature from 303 to 333 K raises rare earth extraction from 20% to 75% at 10 min and at 90 min causes an increase from 80% to 100%. It was found that the dissolution rate of rare earth Y and Eu exhibited the same leaching behavior, which might be because Y and Eu have the same crystal structure as that of YOS. It can be seen that the dissolution curves become parabolic after 10 min with a temperature above 323 K, while at temperatures under 318 K the curves become parabolic until 30 min or longer, which can be ascribed to the faster reaction at higher temperatures. However, it has been reported that the decomposition of hydrogen peroxide will increase apparently at temperature above 323 K.[21] In our experiment, we also observed the generation of oxygen bubbles by the decomposition. As a consequence, the optimal temperature was testified to be 313−323 K, and 313 K was used for subsequent experiments.

3.2.3. Effect of H_2O_2 Concentration. To resolve the effect of hydrogen peroxide concentration on the dissolution, the experiments were performed by varying the initial H_2O_2 concentration in the range of 0.5−2.0 M at 313 K in solutions containing 4 M of hydrochloric acid. While, in the absence of hydrogen peroxide, less than 5% of the rare earths were extracted within 12 h (Figure 2), and hydrogen sulfide was detected. With the increase of H_2O_2 concentration, the dissolution rate of rare earths accelerates considerably as shown in Figure 5. At 1 M of H_2O_2, the rare earths were almost extracted completely after 90 min; at the same time, H_2S was avoided efficiently, and no solid products were detected. Then, $BaCl_2$ was added into the leachate, finding that a large amount of white precipitate was produced, and XRD analyses proved it to be $BaSO_4$, which illustrated that S^{2-} was oxidized to be SO_4^{2-} in the leaching process. When the H_2O_2 concentration was higher than 1 M, the growth of rare earth dissolution rate slows down, and excessive H_2O_2 can lead to waste. As a consequence, the optimal H_2O_2 concentration to the

DOI: 10.1021/acssuschemeng.6b01965
ACS Sustainable Chem. Eng. 2016, 4, 7080−7089

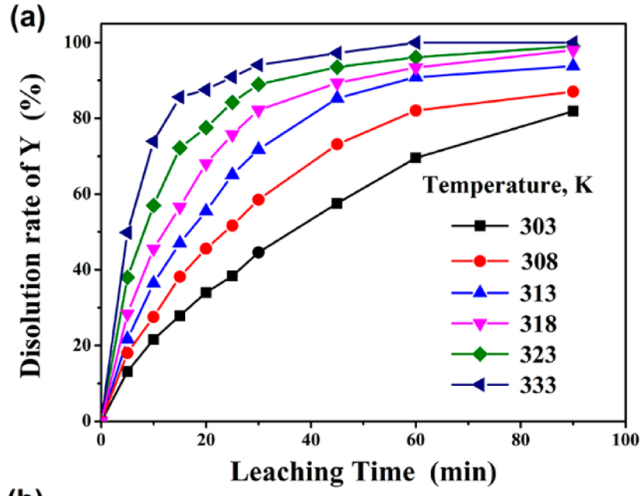

Figure 4. Effect of temperature on the dissolution of YOS: (a) dissolution rate of Y; (b) dissolution rate of Eu.

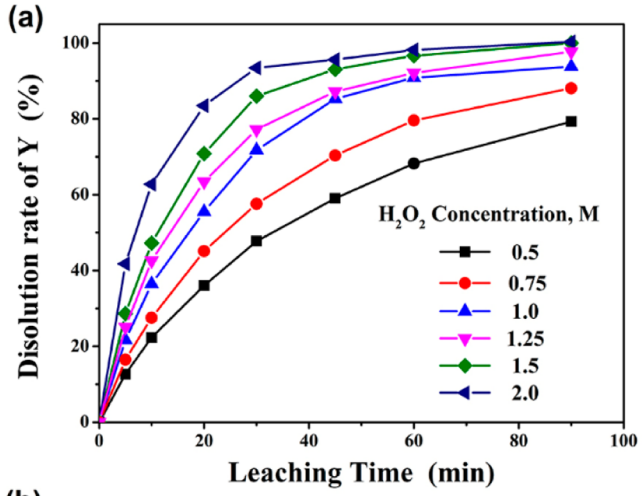

Figure 5. Effect of H_2O_2 concentration on the dissolution of YOS: (a) dissolution rate of Y; (b) dissolution rate of Eu.

dissolution of YOS was testified to be 1−1.5 M, and 1 M was used for subsequent experiments.

3.2.4. Effect of HCl Concentration. The effects of hydrochloric acid concentration on the dissolution were carried out by varying the initial concentration from 1.0 to 5.0 M at 313 K in solution containing 1 M of hydrogen peroxide, and the results are shown in Figure 6. Interestingly, at below 3 M of HCl, there was a negative effect on the rare earth dissolution with increasing the concentration. The leaching behavior was remarkably enhanced with the increasing of HCl concentration from 3 to 5 M. As shown in Figure 6, the dissolution rate of Y and Eu were reduced from 70% to 63% when increasing HCl concentration from 1.0 to 3.0 M within 30 min and then increased to over 90% contrarily at 5 M.

However, different sulfur-containing products with different valences were generated by varying HCl concentration. Figure 7a shows the detection of H_2S employing lead acetate papers in different HCl concentrations, which illustrated that with the increasing of HCl concentration, H_2S was decreased gradually and disappeared at 4.0 M. Elemental sulfur was another main intermediate product at difference HCl concentrations, which was seen by the naked eye, also proved by XRD analyses (Figure S3 in SI-section III). Figure 7b shows the mass distribution of different sulfur-containing products at difference HCl concentrations, where a sulfate radical was measured by barium sulfate precipitation (SI-section II). It was found that with the increase of HCl concentration, the amount of elemental sulfur presented a trend of increasing first and then decreasing. At 3.5 M of HCl concentration, almost all sulfur in YOS was converted to the sulfate radical. Considering the efficiency, reaction complexity, and environment pollution, the optimal HCl concentration was testified to be 3.5−4.5 M, and 4 M should be preferred. Meanwhile, the effect of Cl ions was tested by adding different concentrations of NaCl, and the results illustrated that the effects could be ignored as shown in section IV (Table S2) in the Supporting Information (SI).

3.3. Chemical Reaction Mechanism. Given the above experimental phenomenon, we speculated that different redox reactions occurred driven by HCl concentration. At the optimum conditions, the overall reaction of YOS dissolution in a mixture of hydrogen peroxide and hydrochloric acid medium can be expressed as eq 1.

$$(Y, Eu)_2O_2S + 4H^+ + 4H_2O_2 \rightarrow 2Y^{3+}(Eu^{3+}) + 6H_2O + SO_4^{2-} \quad (1)$$

As shown in Figure 2d and f, single HCl or H_2O_2 cannot dissolve YOS efficiently. In contrast, the complete dissolution of YOS is achieved by the mixture of HCl and H_2O_2. That means the combination of HCl and H_2O_2 shows a synergistic effect on the dissolution. On the basis of the experimental results, the following two reaction mechanisms could be

DOI: 10.1021/acssuschemeng.6b01965
ACS Sustainable Chem. Eng. 2016, 4, 7080−7089

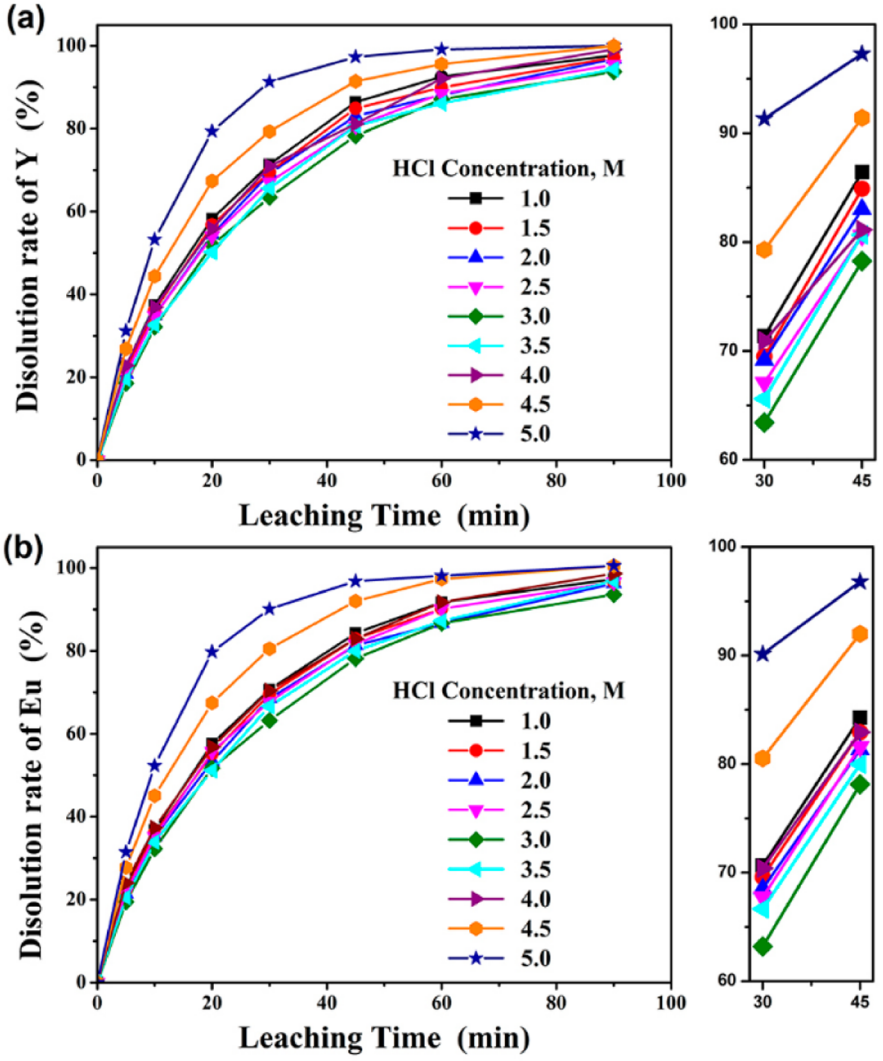

Figure 6. Effect of HCl concentration on the dissolution of YOS: (a) dissolution rate of Y; (b) dissolution rate of Eu.

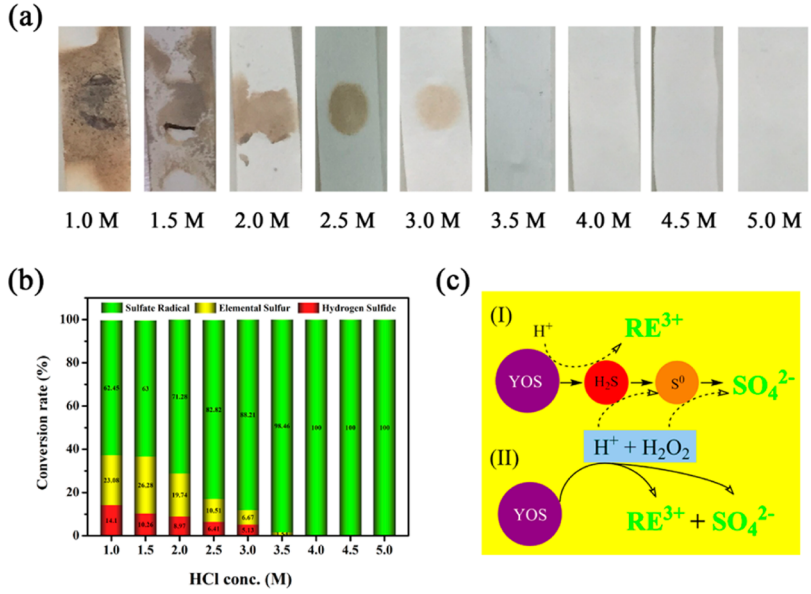

Figure 7. Detection of different sulfur-containing products at different HCl concentrations and reaction mechanism discussion: (a) hydrogen sulfide detection, (b) mass distribution of different sulfur-containing products, and (c) reaction mechanism.

DOI: 10.1021/acssuschemeng.6b01965
ACS Sustainable Chem. Eng. 2016, 4, 7080−7089

assumed (Figure 7c): (I) The overall reaction (eq 1) does not occur in a single reaction step; instead, the reaction should consist of several elementary reactions from step a–c. At the very start, YOS was dissolved by HCl, Y and Eu were released as cations into solution, and H_2S was generated as the first intermediate product (eq 2). However, the dissolution of YOS in HCl is a pretty slow process. Then, H_2O_2 acts as an oxidizing agent (eq 3) which oxidizes H_2S generated in step a to be S^0 (eq 4) and finally to be SO_4^{2-} (eq 5). The oxidization not only avoids the pollution, but more importantly, it keeps on consuming H_2S and promotes the nonoxidative reaction (eq 2) continuously. Particularly, it should be point out that all the elementary reactions simultaneously occurred in the leaching process, instead of in a step-by-step sequence. Thus, no hydrogen sulfide and elemental sulfur were detected at the optimum conditions.

(a) Dissolution of YOS:

$$(Y, Eu)_2O_2S + 6H^+ \rightarrow 2Y^{3+}(Eu^{3+}) + 2H_2O + H_2S \quad (2)$$

(b) Oxidation action of H_2O_2 based on its reduction:

$$H_2O_2 + 2H^+ + 2e^- \rightarrow 2H_2O \quad (3)$$

(c) Reduction action of H_2S:

$$H_2S - 2e^- \rightarrow S^0 + 2H^+ \quad (4)$$

$$S^0 + 4H_2O - 6e^- \rightarrow SO_4^- + 8H^+ \quad (5)$$

(II) However, the oxidative leaching process was also likely to directly occur as eq 6. Definitely, the hydrogen ion concentration can increase the redox potential of hydrogen peroxide,[22,23] that is to say the more hydrogen ions there are, the stronger the oxidation of hydrogen peroxide will be. While in lower HCl concentration, side reactions (eq 3) occurred according to experiments. At higher HCl concentration, the oxidation of H_2O_2 is enough to oxidize the divalent S in YOS to be SO_4^{2-} into solution, and the synergic effect of H^+ and H_2O_2 can take place as shown in eq 1 directly in one step.

$$(Y, Eu)_2O_2S + 6H^+ + H_2O_2 \rightarrow 2Y^{3+}(Eu^{3+}) + 4H_2O + S \quad (6)$$

3.4. Kinetics Study. To further understand the mechanism of a leaching system, it is important to investigate the leaching kinetics of the dissolution reaction. The dissolution of YOS by hydrochloric acid and hydrogen peroxide is a typical liquid–solid reaction, which can be expressed as follows:

$$A_{fluid} + B_{particle} \rightarrow product \quad (7)$$

Generally, the kinetics of a liquid–solid reaction is explained by the shrinking core model, and the following three kinetic equations can be applied for different rate-controlling steps.[24–26]

$$x = k_l t \quad (8)$$

$$1 - (1 - x)^{1/3} = k_c t \quad (9)$$

$$1 - \frac{2}{3}x - (1 - x)^{2/3} = k_d t \quad (10)$$

where x is the extraction rate of rare earths, and k_l, k_c, and k_d are the apparent rate constants which are calculated from eqs 8–10, respectively.

If the leaching process is controlled by diffusion through a liquid boundary layer, the integrated rate equation will be followed with eq 8. If the leaching process is controlled by a chemical reaction, the integrated rate equation will be followed by eq 9. If the leaching process is controlled by diffusion through the product layer, the integrated rate equation will be followed by eq 10.

In the present study, the dissolution involves a chemical reaction between YOS and leaching reagents. The effect of stirring speed has already indicated that the reaction was not controlled by film diffusion. Therefore, the chemical reaction controlled model and diffusion through the product layer controlled model were considered for the kinetics study. The dissolution rate of yttrium (the main rare earth content of YOS) in the temperature range from 303 to 323 K given in Figure 4 was plotted against reaction time according to eqs 9 and 10, respectively. As shown in Figure 8, the chemical reaction controlled model gives a more straight line, which indicates that eq 9 could be more suitable for demonstrating the kinetics of this leaching process.

Moreover, it has been commonly accepted that a chemical controlled leaching process is strongly dependent on temperature, and the reaction rate constant can be determined by the Arrhenius equation:

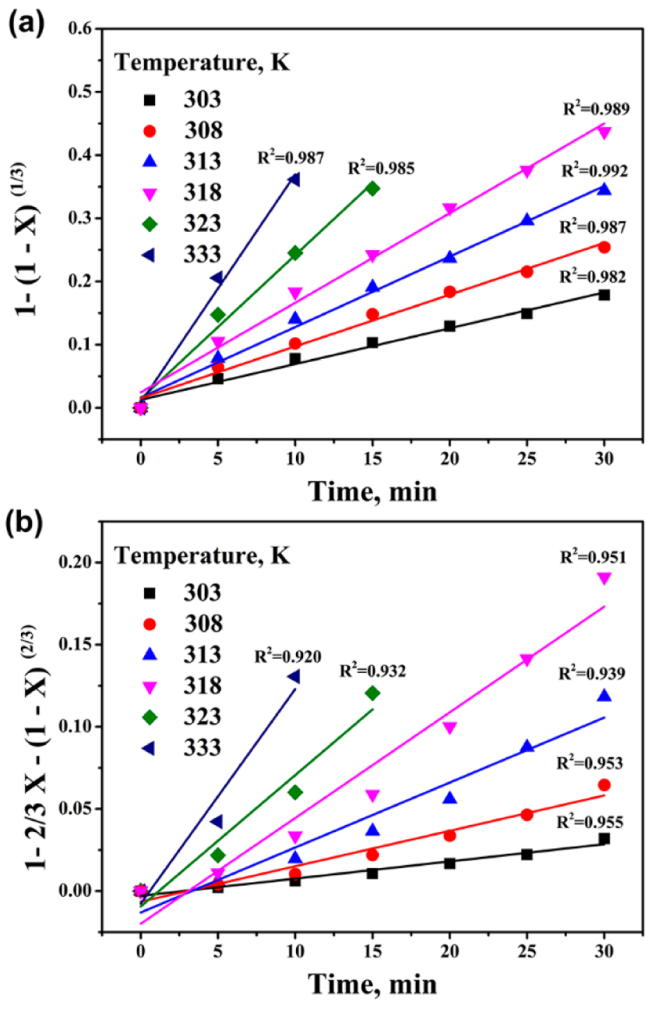

Figure 8. YOS dissolution ratio versus time at various temperatures fitted by (a) a chemical reaction model equation and (b) a diffusion through product layer model equation.

DOI: 10.1021/acssuschemeng.6b01965
ACS Sustainable Chem. Eng. 2016, 4, 7080–7089

$$k = A_0 \cdot C^n \cdot \exp\left(-\frac{E_a}{RT}\right) \quad \text{or}$$

$$\ln k = \ln A_0 + n \ln C - \frac{E_a}{R} \times \frac{1}{T} \tag{11}$$

where E_a is the apparent activation energy, A_0 is the pre-exponential factor, C is the initial concentration of the lixiviant (HCl or H_2O_2), n is the reaction order of the lixiviant which can be determined by experiments, R is the universal gas constant, and T is the absolute temperature.

Subsequently, the natural logarithm of the reaction rate constant ($\ln k$) at different temperatures calculated by the chemical reaction control model against the reciprocal of absolute temperature ($1/T$) are ploted in Figure 9, and the

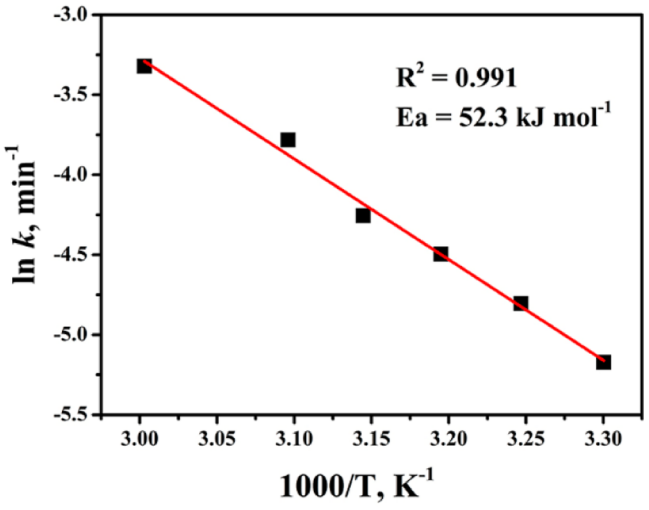

Figure 9. Arrhenius plot for the dissolution of YOS.

apparent activation energy E_a of the reaction was calculated as 52.3 kJ/mol based on eq 11. The apparent activation energy has a value >40 kJ/mol, which also indicates a chemical reaction control mechanism.[26]

In order to further understand the effect of H_2O_2, the data from Figure 5a were analyzed according to the chemical reaction model equation $1 - (1 - x)^{1/3} = kt$, and the rate constants were determined. Then, a plot of $\ln k$ and $\ln$ [H_2O_2 conc.] were obtained. As can be seen in Figure 10a, the dissolution rate is found to increase with H_2O_2 concentration. The linear relationship in Figure 10b with a correlation coefficient of 0.991 illustrates that H_2O_2 has a positive influence on the chemical reaction rate and does not change the chemical reaction, which was in conformity with the experiment results; before that, no H_2S and elemental sulfur were detected even at lower H_2O_2 concentration. The order of the leaching reaction was found to power 0.82 of H_2O_2 concentration.

Similarly for hydrochloric acid concentration, the data from Figure 6a were analyzed according to the chemical reaction model equation $1 - (1 - x)^{1/3} = kt$, and the rate constants were determined, and a plot of $\ln k$ and $\ln$ [HCl conc.] was obtained. As can be seen in Figure 11b, −0.09 reaction order was found for HCl concentration from 1.0 to 3.5 M, while for concentration from 3.5 to 5.0 M, the reaction order was found to be 2.13. According to the experimental phenomenon, elemental sulfur was detected when HCl concentration was lower than 3.5 M. The change in dissolution rate can be

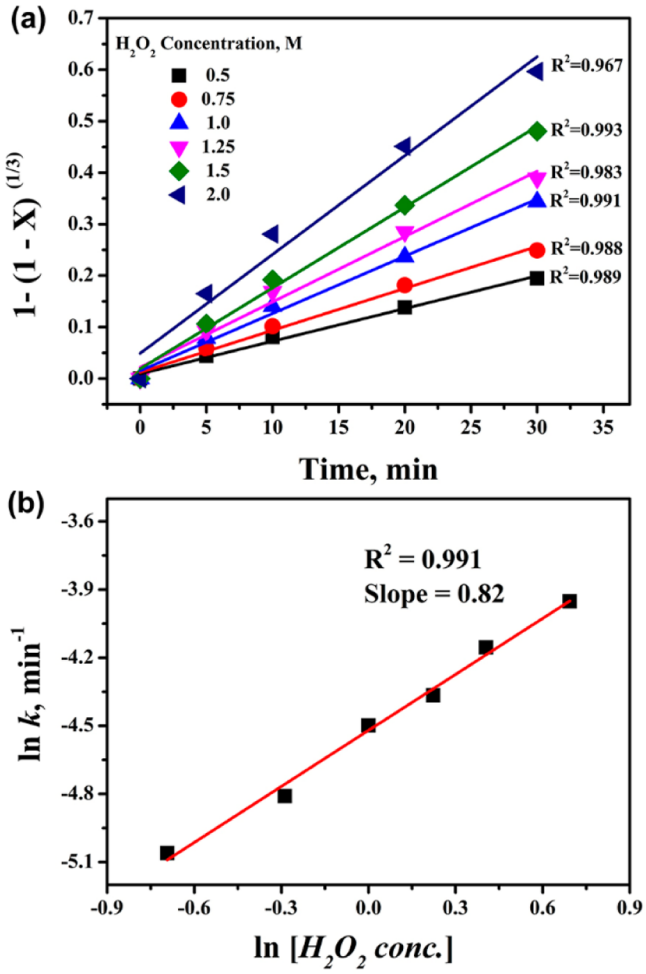

Figure 10. Plot of (a) the variation of $1 - (1 - x)^{1/3}$ with time for various H_2O_2 concentrations and (b) determination of the reaction order with respect to [H_2O_2 conc.].

explained by the product of elemental sulfur, which changes the rate controlling step to diffusion of the reacting species through the sulfur film formed on the surface of the pellets, which caused a limitation on the overall reaction rate.[27,28] When the HCl concentration was higher than 3.5 M, the sulfate ion was almost the single product, and elemental sulfur disappeared. The leaching process was transferred to complete the chemical controlling step. The reaction orders for H_2O_2 and HCl were 0.82 and 2.13, respectively, which means that HCl has a more significate effect on YOS dissolution. This is likely due to the fact that HCl not only supplies the hydrogen ion but also acts as an auxiliary reagent for the oxidation behavior of H_2O_2.

According to eqs 9 and 11, the kinetic equation can be expressed as follows:

$$1 - (1 - x)^{1/3} = k_c t = A_0 \cdot C_{[H_2O_2]}^{n_1} \cdot C_{[HCl]}^{n_2} \cdot \exp\left(-\frac{Ea}{RT}\right) \cdot t \tag{12}$$

where n_1 is the reaction order of H_2O_2 determined by experiments, and n_2 is the reaction order of HCl determined by experiments.

As calculated employing the chemical reaction model equation and the Arrhenius equation, the apparent activation energy was obtained as 52.3 kJ/mol, and the reaction orders of H_2O_2 and HCl were 0.83 and 2.13, respectively. A_0 values were

DOI: 10.1021/acssuschemeng.6b01965
ACS Sustainable Chem. Eng. 2016, 4, 7080−7089

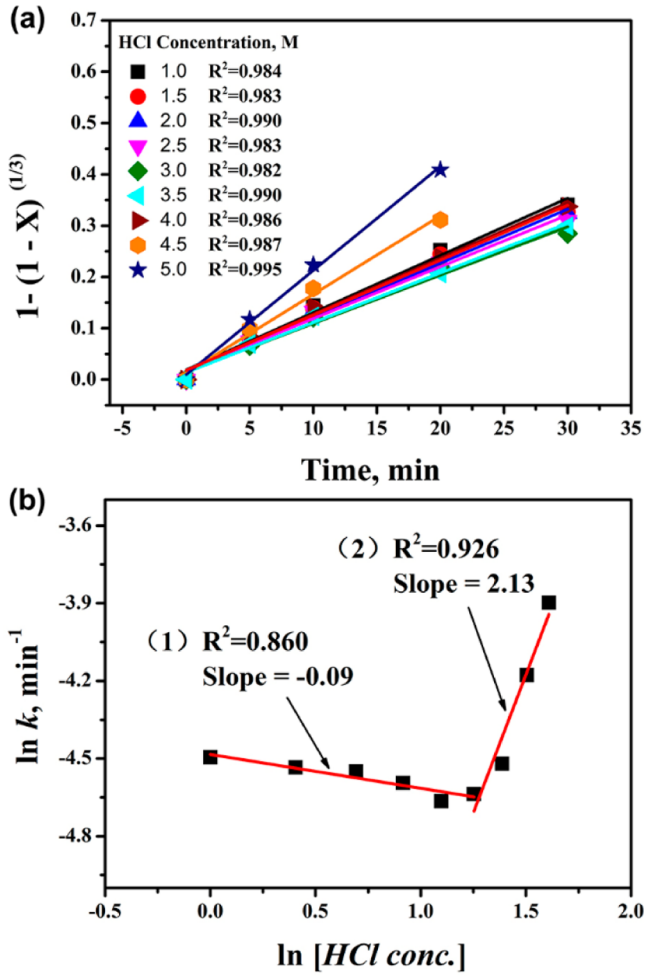

Figure 11. Plot of (a) the variation of $1 - (1 - x)^{1/3}$ with time for various HCl concentrations and (b) determination of the reaction order with respect to [HCl conc.].

calculated from the intercepts of lines given in Figure 9, Figure 10b, and Figure 11b as 3.13×10^5, 3.10×10^5, and 3.34×10^5, respectively. The average of these three values is 3.19×10^5, which is used in the kinetic equation.[29] As a result, the kinetics equation for rare earth extraction by oxidative leaching in this study can be described as

$$1 - (1 - x)^{1/3} = 3.19 \times 10^5 \cdot C_{[H_2O_2]}^{0.82} \cdot C_{[HCl]}^{2.13} \cdot \exp\left(-\frac{523,000}{8.314T}\right) \cdot t \quad (13)$$

3.5. Dissolution of Waste CRT Phosphor. Having established the optimal parameters for the dissolution of pure YOS, our next goal was to investigate the practical application of optimum on the real waste CRT phosphor (enriched WCP). The experimental results show that the rare earths in enriched WCP were completely dissolved after stirring in lixiviant containing 4 M of HCl and1 M of H_2O_2 at 313 K for 90 min. However, the kinetics of oxidative leaching of pure-YOS and ER-WCP were compared, a plot of $1 - (1 - x)^{1/3}$ vs time was obtained, and the reaction rate constants (slop) were determined. As shown in Figure 12, the slope of YOS and ER-WCP are 0.0083 and 0.0075, indicating that the leaching rate presents a small slow down for WCP compared with pure

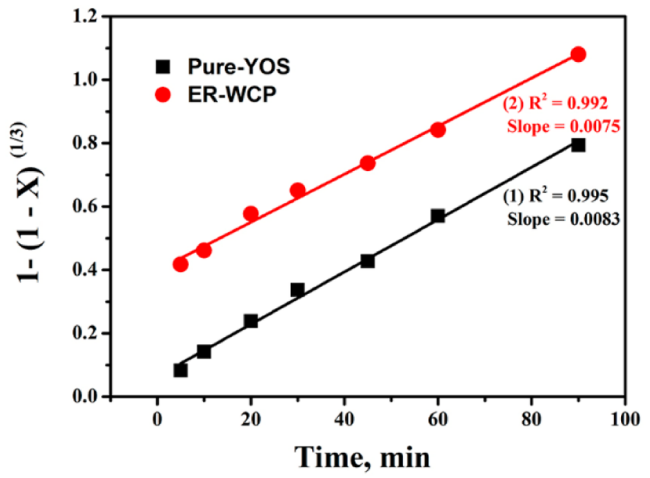

Figure 12. Leaching kinetics of pure-YOS and ER-WCP at optimal conditions.

YOS. This is likely due to the presence of impurities and uneven particle size, which causes a delay in leaching process.

3.6. Selective Precipitation of RE Salts. Having got the resulting rare earth solution of ER-WCP after leaching and filtration, we explored the selective precipitation of rare earths. Oxalic acid was employed as the precipitation reagent because it is a commonly used and effective rare earth precipitation reagent[30] with a high purification rate for impurities such as zinc, aluminum, silicon, and calcium, which are the main impurities in the leaching solution. Oxalic acid with a concentration of 100 g/L was added gradually into the RE leaching solution, and a pH of 1.8−2.0 was adjusted by adding ammonium hydroxide gradually, so that the rare earth oxalate would be generated and precipitated. After complete precipitation for 12−15 h at room temperature, the rare earth oxalate was filtrated and washed several times using dilute oxalic acid, resulting in >99.5% yield of $(RE)_2(C_2O_4)_3$ being recycled. Later, the obtained RE oxalates were calcined at 950 °C for 2 h, and a final product of rare earth oxides were obtained. The XRD pattern of the RE oxides in Figure 13a indicates a well crystallized $(Y_{0.95}Eu_{0.05})_2O_3$ (PDF# 25-1011), which can be used as a solid reagent or directly used as fluorescent material (a kind of red phosphor). The SEM image in Figure 13b shows that the product particles are uniformly distributed with an average diameter of 5 μm. The energy dispersive spectroscopy analysis (EDS) indicates the main elemental compositions of the particles are Y, Eu, and O, which correspond to the XRD results. The purity of RE oxides product was analyzed by ICP-OES resulting in >99%.

4. CONCLUSIONS

An efficient and green process for the recovery of rare earths from waste CRT phosphors was proposed in this work, and the following conclusions can be summarized.

(1) A mixed lixiviant containing hydrochloric acid and hydrogen peroxide was identified as the most suitable leaching agent for YOS dissolution due to the synergistic effect. Temperature, H_2O_2 concentration, HCl concentration, and leaching time had a significant influence on dissolution of YOS. Stirring was indeed necessary for the dissolution, but the leaching process was independent of stirring speed. The optimal leaching conditions for complete dissolution of YOS were obtained as follows: stirring speed 600 rpm, temperature

DOI: 10.1021/acssuschemeng.6b01965
ACS Sustainable Chem. Eng. 2016, 4, 7080−7089

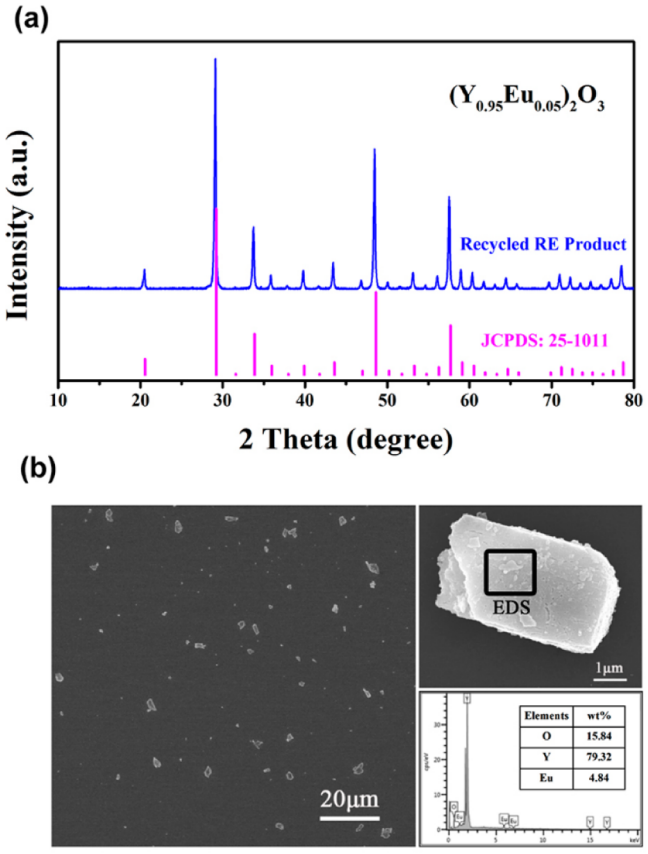

Figure 13. Characteristics of rare earth oxides product: (a) XRD pattern and (b) SEM images and EDS analysis.

313 K, 1 M of H_2O_2, 4 M of HCl, and leaching time 90 min. The optimal conditions were proved to be feasible in the real process.

(2) The leaching reaction equation was expressed, and RE^{3+} and SO_4^{2-} were found to be the main reaction products. Hydrochloric acid had the most important role on the redox reaction in the leaching of YOS, and no other side-reactions occurred when the HCl concentration was more than 3.5 M. Reaction mechanism analyses indicate that HCl not only supplies hydrogen ion but also acts as an auxiliary reagent for the oxidation behavior of H_2O_2 in the dissolution process.

(3) According to kinetic study using the shrinking core model, the leaching process was controlled by the chemical reaction. The apparent activation energy was 52.3 kJ/mol, and the reaction orders for H_2O_2 and HCl were 0.82 and 2.13, respectively. The kinetics equation for rare earths extraction by oxidative leaching can be described as $1 - (1 - x)^{1/3} = 3.19 \times 10^5 \cdot C_{[H_2O_2]}^{0.82} \cdot C_{[HCl]}^{2.13} \cdot t$. It was also found that the leaching rate for WCP slows down slightly compared with that of pure YOS, which can be ascribed to the presence of impurities and uneven particle size.

$$\exp\left(-\frac{523,000}{8.314T}\right)\cdot t$$

(4) The oxalate precipitation process was further employed for the recovery of rare earths from the leaching solution. The RE recovery rate is as high as 99.5%, and a well crystallized RE oxides product can be obtained with a purity of 99% and an average diameter of 5 μm.

■ ASSOCIATED CONTENT

Supporting Information

The Supporting Information is available free of charge on the ACS Publications website at DOI: 10.1021/acssuschemeng.6b01965.

Detailed description of raw materials (XRD and XRF analysis) and provides the detecting results of sulfate radical and elemental sulfur in leaching processes and results of the effect of Cl ions on dissolution (PDF)

■ AUTHOR INFORMATION

Corresponding Authors

*(Y.W.) Tel: +86-10-67396234. Fax: +86-10-67396234. E-mail: wuyufeng3r@126.com.

*(J.Y.) No. 100, PingleyuanStreet, Chaoyang District, Beijing, 100124, China. E-mail: jyu@bjut.edu.cn.

Notes

The authors declare no competing financial interest.

■ ACKNOWLEDGMENTS

This research was financially supported by Beijing Nova Program (Z1511000003150141) and Capital Resources Recycling Materials Technology Collaborative Innovation Center Program (009000546616016).

■ REFERENCES

(1) Guo, C.; Luan, L.; Chen, C.; Huang, D.; Su, Q. Preparation of $Y_2O_2S:Eu^{3+}$ phosphors by a novel decomposition method. *Mater. Lett.* **2008**, *62*, 600−602.

(2) Behrendt, M.; Szczodrowski, K.; Mahlik, S.; Grinberg, M. High pressure effect on charge transfer transition in Y2O2S:Eu3+. *Opt. Mater.* **2014**, *36*, 1616−1621.

(3) Lo, C. L.; Duh, J. G.; Chiou, B. S. Low-voltage cathodoluminescence properties of the Y_2O_2S: Eu red light emitting phosphor screen in field-emission environments. *J. Electrochem. Soc.* **2002**, *149*, H129−H133.

(4) Sovers, O. J. Fluorescence of Trivalent-Europium-Doped Yttrium Oxysulfide. *J. Chem. Phys.* **1968**, *49*, 4945.

(5) Zhang, Q.; Fu, Y.; Wu, Y.; Zhang, Y.; Zuo, T. Low-Cost Y-Doped TiO2 Nanosheets Film with Highly Reactive {001} Facets from CRT Waste and Enhanced Photocatalytic Removal of Cr(VI) and Methyl Orange. *ACS Sustainable Chem. Eng.* **2016**, *4*, 1794−1803.

(6) Yang, Y.; Williams, E. Logistic model-based forecast of sales and generation of obsolete computers in the U.S. *Technol. Forecast. Soc.* **2009**, *76*, 1105−1114.

(7) Gong, Y.; Tian, X.; Wu, Y.; Tan, Z.; Lv, L. Recent development of recycling lead from scrap CRTs: A technological review. *Waste Manage.* **2015**, DOI: 10.1016/j.wasman.2015.09.004.

(8) Resende, L. V.; Morais, C. A. Study of the recovery of rare earth elements from computer monitor scraps − Leaching experiments. *Miner. Eng.* **2010**, *23*, 277−280.

(9) Resende, L. V.; Morais, C. A. Process development for the recovery of europium and yttrium from computer monitor screens. *Miner. Eng.* **2015**, *70*, 217−221.

(10) Dexpert-Ghys, J.; Regnier, S.; Canac, S.; Beaudette, T.; Guillot, P.; Caillier, B.; Mauricot, R.; Navarro, J.; Sekhri, S. Re-processing CRT phosphors for mercury-free applications. *J. Lumin.* **2009**, *129*, 1968−1972.

(11) Lee, C.; Hsi, C. Recycling of Scrap Cathode Ray Tubes. *Environ. Sci. Technol.* **2002**, *36*, 69−75.

(12) Bian, Y.; Guo, S.; Jiang, L.; Liu, J.; Tang, K.; Ding, W. Recovery of Rare Earth Elements from NdFeB Magnet by VIM-HMS Method. *ACS Sustainable Chem. Eng.* **2016**, *4*, 810−818.

DOI: 10.1021/acssuschemeng.6b01965
ACS Sustainable Chem. Eng. 2016, 4, 7080−7089

(13) Binnemans, K.; Jones, P. T.; Blanpain, B.; Van Gerven, T.; Yang, Y.; Walton, A.; Buchert, M. Recycling of rare earths: a critical review. *J. Cleaner Prod.* **2013**, *51*, 1−22.
(14) Wu, Y.; Yin, X.; Zhang, Q.; Wang, W.; Mu, X. The recycling of rare earths from waste tricolor phosphors in fluorescent lamps: A review of processes and technologies. *Resour. Conserv. Recycl.* **2014**, *88*, 21−31.
(15) Innocenzi, V.; De Michelis, I.; Ferella, F.; Beolchini, F.; Kopacek, B.; Vegliò, F. Recovery of yttrium from fluorescent powder of cathode ray tube, CRT: Zn removal by sulphide precipitation. *Waste Manage.* **2013**, *33*, 2364−2371.
(16) Antonijević, M. M.; Janković, Z. D.; Dimitrijević, M. D. Kinetics of chalcopyrite dissolution by hydrogen peroxide in sulphuric acid. *Hydrometallurgy* **2004**, *71*, 329−334.
(17) Aydogan, S. Dissolution kinetics of sphalerite with hydrogen peroxide in sulphuric acid medium. *Chem. Eng. J.* **2006**, *123*, 65−70.
(18) Antonijević, M. M.; Janković, Z. D.; Dimitrijević, M. D. Kinetics of chalcopyrite dissolution by hydrogen peroxide in sulphuric acid. *Hydrometallurgy* **2004**, *71*, 329−334.
(19) Adebayo, A. O.; Ipinmoroti, K. O.; Ajayi, O. Dissolution kinetics of chalcopyrite with hydrogen peroxide in sulphuric acid medium. *Chem. Biochem. Eng. Q.* **2003**, *17*, 213−218.
(20) Antonijevic, M. M.; Dimitrijevic, M.; Jankovic, Z. Leaching of pyrite with hydrogen peroxide in sulphuric acid. *Hydrometallurgy* **1997**, *46*, 71−83.
(21) Dimitrijevic, M.; Antonijevic, M. M.; Jankovic, Z. Kinetics of pyrite dissolution by hydrogen peroxide in perchloric acid. *Hydrometallurgy* **1996**, *42*, 377−386.
(22) Cotton, F. A. *Advanced Inorganic Chemistry*, 6th ed.; Wiley: New York, 1999.
(23) Szymczycha-Madeja, A. Kinetics of Mo, Ni, V and Al leaching from a spent hydrodesulphurization catalyst in a solution containing oxalic acid and hydrogen peroxide. *J. Hazard. Mater.* **2011**, *186*, 2157−2161.
(24) Randhawa, N. S.; Gharami, K.; Kumar, M. Leaching kinetics of spent nickel−cadmium battery in sulphuric acid. *Hydrometallurgy* **2016**, *165*, 191−198.
(25) Wu, D.; Wen, S.; Deng, J. Leaching kinetics of cerussite using a new complexation reaction reagent. *New J. Chem.* **2015**, *39*, 1922−1929.
(26) Wadsworth, M. E.; Miller, J. D. Hydrometallurgical Processes. In *Rate Processes of Extractive Metallurgy*; Springer: New York, 1979.
(27) Biswas, A. K.; Mohan, N. P. Kinetics of dissolution of copper (II) sulphide in aqueous sulphuric acid solutions. *J. Appl. Chem. Biotechnol.* **1971**, *21*, 15−18.
(28) Aydoğan, S.; Erdemoğlu, M.; Uçar, G.; Aras, A. Kinetics of galena dissolution in nitric acid solutions with hydrogen peroxide. *Hydrometallurgy* **2007**, *88*, 52−57.
(29) He, G.; Zhao, Z.; Wang, X.; Li, J.; Chen, X.; He, L.; Liu, X. Leaching kinetics of scheelite in hydrochloric acid solution containing hydrogen peroxide as complexing agent. *Hydrometallurgy* **2014**, *144−145*, 140−147.
(30) Yang, X.; Zhang, J.; Fang, X. Rare earth element recycling from waste nickel-metal hydride batteries. *J. Hazard. Mater.* **2014**, *279*, 384−388.

DOI: 10.1021/acssuschemeng.6b01965
ACS Sustainable Chem. Eng. 2016, 4, 7080−7089